

BEAM DYNAMICS OF NOVEL HYBRID ION MASS ANALYSERS

R.B. Appleby, T. Rose*, The University of Manchester and the Cockcroft Institute, UK
 K. Richardson, M. Green, P. Nixon, Waters Corporation, UK

Abstract

Fourier transform (FT) mass spectrometers achieve high resolution using relatively long transient times by trapping ions and measuring the frequency of their motion (inductively) inside an electrostatic potential. By contrast, time-of-flight (ToF) mass spectrometers measure the time of flight between an initiation pulse and contact with a destructive detector positioned on a plane of space focus after flying along a predetermined route. These devices have relatively short flight times and, generally, lower resolution. A class of hybrid analysers have been proposed and studied, utilising a quadro-logarithmic potential to reflect ions multiple times past an inductive detector, with the potential for the short transient of ToF devices - and the high resolution of FT devices. In this paper we compute the ion dynamics inside such devices, tracking bunches of ions and studying induced signals.

INTRODUCTION

The novel device studied in this paper operates in a similar manner to Orbitrap mass spectrometers [1] - confining ions in circular orbits using their angular momentum, using a quadratic axial potential to force ions into simple harmonic motion along the axis perpendicular to the orbital motion, and measuring induced current. The potential is supported by a series of segmented rings, held at the voltage described by the field at the centre of each electrode so that the region contained relaxes to the desired potential. The oscillation frequency of ions inside the device, used to calculate their mass-to-charge, is measured via the differential image current produced by grounded electrodes located at the central plane of the device. This differs to the Orbitrap, wherein the image current is recorded over the entire oscillation of ions [2]. The signal from this new device takes the form of sharp pulses corresponding to when ions pass the detectors, which, compared to the signal from an Orbitrap, may offer higher mass-to-charge resolution per unit time. The oscillation frequency (and therefore mass measurement) is affected by the accuracy of the electrostatic potential produced by the device, which is affected by the segmentation, the detector electrodes, and the errors in voltage applied to the electrodes, which arise from source fluctuations and component impedance errors.

* Corresponding author, toby.rose@postgrad.manchester.ac.uk

OVERVIEW OF THE DEVICE

Producing the Potential

The electrostatic potential used takes a quadro-logarithmic form,

$$U(r, z) = \frac{k}{2} \left(z^2 - \frac{r^2}{2} \right) + b_0 \ln \left(\frac{r}{r_0} \right) + b_1, \quad (1)$$

where r and z are the radial and axial components of a cylindrical coordinate system, and k , b_0 , r_0 , and b_1 are parameters which define the shape of the potential. It is supported by a series of adjacent pairs of concentric ring electrodes, with segmented caps at each end. A representative diagram is shown in Figure 1.

The bulk of the analyser spans 1.1 m axially, made from 110 pairs of 8 mm wide electrodes separated by 2 mm. The inner electrodes have radius 20 mm and the outer electrodes have radius 100 mm. The caps are a series of 8 concentric annular electrodes, 8 mm thick with 2 mm separation, located 2 mm from the edge the bulk of the device.

Ion Motion

Richardson *et al.* [3] have described and classified the solutions to the equations of motion for the quadro-logarithmic potential. Axial and orbital motion are decoupled and the useful results are shown below.

Axial motion The axial motion has well known solutions when $qk > 0$, which describe confined sinusoidal oscillations with angular frequency given by

$$\omega = \sqrt{\frac{qk}{m}}. \quad (2)$$

Orbital motion The important case of stably bound circular orbits occurs when the parameters of the potential satisfy

$$b_0 > 2\sqrt{k\Delta U}R_0, \quad (3a)$$

and

$$b_0 = \frac{k}{2}R_0^2 + 2\Delta U, \quad (3b)$$

where ΔU is the potential difference applied to accelerate ions into the device, and R_0 is the radius of injection.

IMPACT OF SEGMENTATION

The segments used to create the potential are finite in size and have to be held at a static voltage. This creates a deviation to the ideal potential which perturbs ion trajectories, which will affect the signal produced and ultimately performance. To measure these effects, a device is simulated in SIMION 8.1 [4] [5], using the parameters $k = 80000 \text{ Vm}^{-2}$,

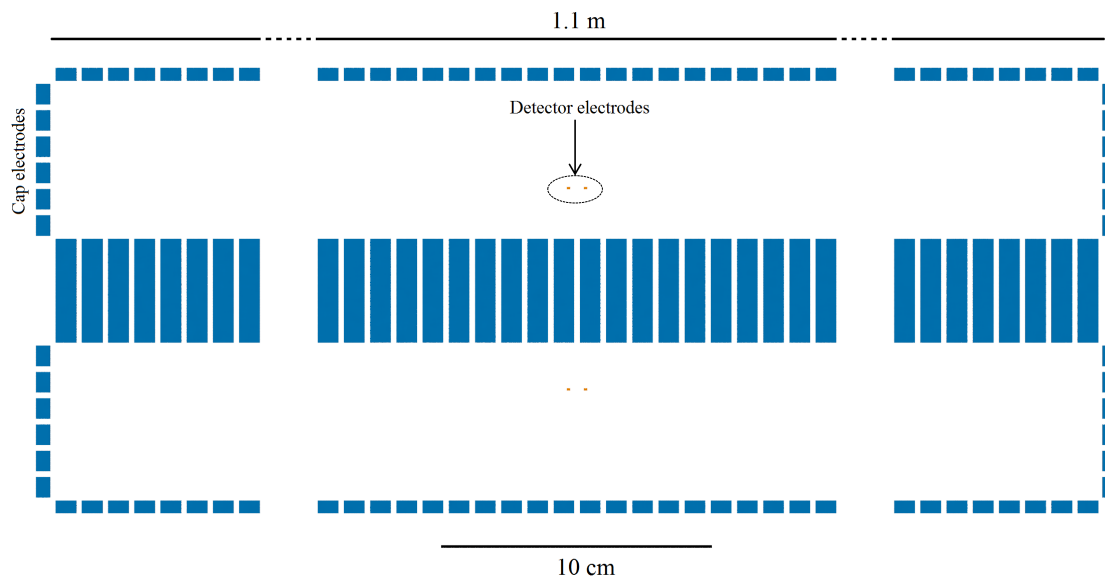


Figure 1: Cross section of the analyser in the (r, z) plane. The length shown is in reality shorter than the proposed device in order to show the end caps and detector electrodes. The detectors sit at radius 39 mm, 1.5 mm inside the target radius for ion orbits to maximise signal amplitude whilst allowing for some deviation of trajectories.

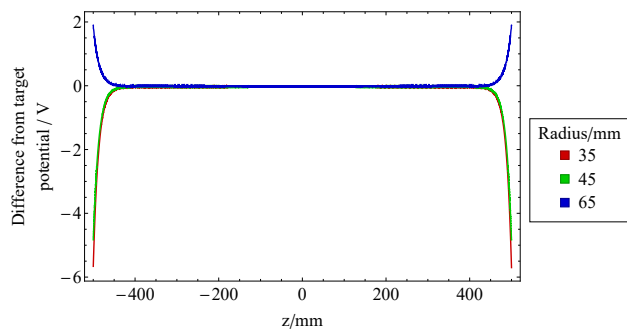


Figure 2: Difference in axial potential at various radii. The small fluctuations that can be seen are due to the finite difference method's convergence objective of 0.0001% being satisfied.

$b_0 = 2469$ V, $r_0 = 64$ mm, and $b_1 = -1253$ V, so that ions injected at $R_0 = 41.5$ mm with kinetic energy $\Delta U = 1200$ V maintain circular orbits. Each electrode is set to the voltage described by the potential at the centre of the face of each electrode, and the resultant potential is recorded.

The sign and magnitude of the axial deviation, Figure 2, depends on where the trace lines up on the cap electrodes, due to the fact that the potential of the cap electrode only matches at the centre of the inner face. A similar effect is present in the radial field, which penetrates into the bulk of the device, so has to be corrected for by adjusting all of the inner electrodes by -8 V and all outer electrodes by +1 V.

Effects of the Detector Electrodes

The detector electrodes are two rings of outer radius 39 mm with axial width 1.5 mm and depth 0.75 mm, centred

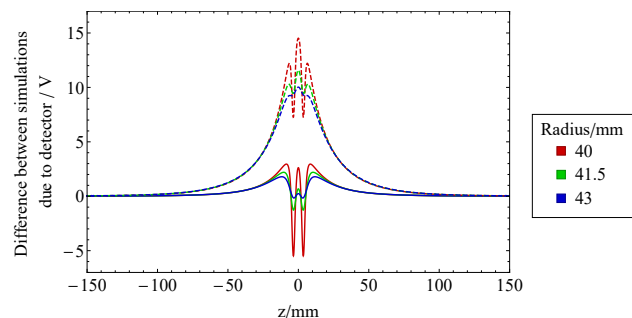


Figure 3: Deviation to potential caused by detectors, and the effects of offsetting the non-detector electrodes by $\Phi_{\text{det}} = 0$ V (Dashed) and $\Phi_{\text{det}} = 15$ V (Solid line).

at $z = \pm 3.5$ mm. The value of the constant b_1 in equation 1 is set to 1253 V so that they can be held at ground. To minimise field error in the range $40 \leq r/\text{mm} \leq 43$, where ions are likely to fly, the entire device except for the detectors is floated by an offset, Φ_{det} . The resultant difference between these two models and the model without a detector is plotted in Figure 3.

IMPACT OF MANUFACTURING DEFECTS AND VOLTAGE FLUCTUATIONS

This device is designed with the intent to be insensitive to physical geometry defects - the large distance between electrodes and ion path allows for the field errors due to the segmentation of the device to relax, as well as errors due to mechanical defects such as misshapen electrodes and construction defects. Deviations in the potential will more likely come from the effects of voltage supply errors, which depend

Content from this work may be used under the terms of the CC BY 3.0 licence (© 2019). Any distribution of this work must maintain attribution to the author(s), title of the work, publisher, and DOI

entirely on the electronics used. In this example, the device will be simulated as if all electrodes except the detectors are supplied by a single 20 kV source using potential divider circuits in parallel to modulate voltages, with a consistent error on supplied voltage, $\sigma_{\text{supp.}}$, and an individual error on each electrode of $\sigma_{\text{el.}}$.

As electrostatic fields obey the superposition principle, a static source offset will deviate all electrodes by the same percentage, so the potential created will have the same percentage offset. When the voltage deviation takes the form of a random error, this relationship still holds to give the relationship

$$\frac{\sigma_U(r,z)}{U(r,z)} = \frac{\sigma_V}{V}, \quad (4)$$

where σ_U is the uncertainty in the produced field, U , and σ_V/V is the fractional error in supply voltage. A range of devices are simulated, in which each electrode has a random Gaussian variate added to it. The resultant potential will also have random deviations that relax towards the centre.

DEVIATIONS TO ION MOTION

The deviations to axial frequency, which effects mass measurement, as well as maximum acceptable errors before trajectories of ions will not pass the detector in a manner suitable for producing a mass spectrum are computed. The effect of a static voltage error on mass measurement can be corrected for by using reference compounds of known mass in an experiment to calibrate the mass scale, or by probing the field / measuring the voltages applied to find the effective value for k . Similarly, the input conditions of ions can be altered slightly to satisfy the equations 3a and 3b for the deviated potential.

The random deviations will affect ion motion in a similar manner, however the effects change in size over the length of the device in a random manner and will cause uncorrectable effects on ion motion. Ions are created at $z_0 = -500$ mm, $R_0 = 41.5$ mm with kinetic energy $\Delta U = 1200$ V angled perpendicularly to the radius, with deviations in position and velocity consistent with having been thermalised at 300 K. To assess axial motion, the frequency of motion for known masses of ion is measured and the percentage deviation in angular axial frequency is measured for bunches of 200 ions. This is shown in Figure 4.

A proportional relationship fitted to this has equation $\frac{\sigma_{\omega}}{\omega} = 0.415 \frac{\sigma_{\text{el.}}}{V}$. The assessment of tolerable errors needs to be made in terms of ultimate device performance. The angular eccentricity is used as one measure of orbital motion, and is defined, in this paper as

$$\alpha = \cos^{-1} \left(\frac{\bar{r}_{\text{min}}}{\bar{r}_{\text{max}}} \right), \quad (5)$$

where subscripts min / max refer to the minimum / maximum radius of the mean ion position in a bunch, \bar{r} , respectively. The typical radial spread of ions is the time average of the standard deviation of ion radius over an entire transient.

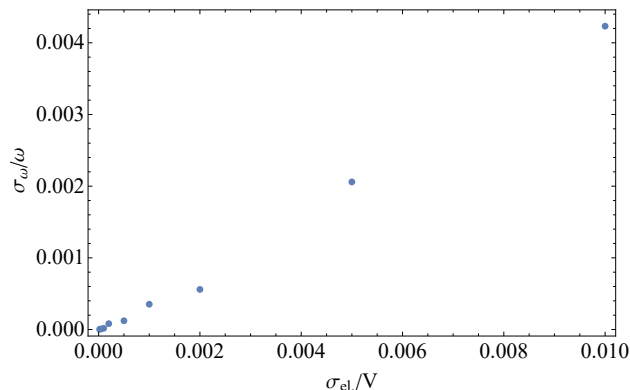


Figure 4: Fractional deviation to oscillation frequency as a function of $\frac{\sigma_{\text{el.}}}{V}$. A contemporary circuit would have approximately 0.5% to 1% error ($0.005 \leq \frac{\sigma_{\text{el.}}}{V} \leq 0.01$).

This radial motion affects the signal strength and consistency - an ion passing the detectors at a larger radius will produce a smaller signal than one passing closer, and can be seen in the peak-to-peak signal strength variation present in Figure 5, the signal produced when $\sigma_{\text{el.}} = 0.7\%$.

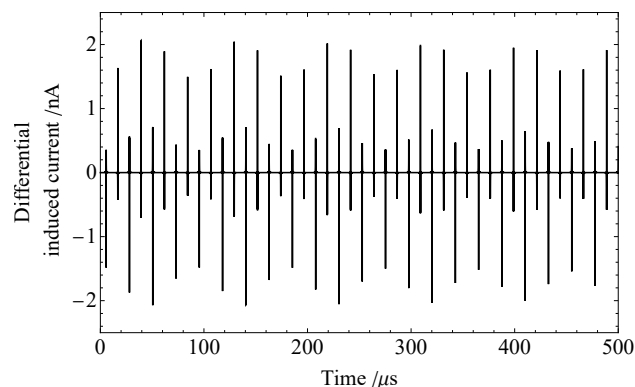


Figure 5: Differential signal induced by 250 ions of mass 100 Da, unit charge and $\sigma_{\text{el.}} = 0.7\%$

CONCLUSIONS

We have shown that the segmented construction can produce a quadro-logarithmic potential accurate enough to confine ions and for the induced current on a pair of in-field detector electrodes produce a periodic signal for use in mass spectrometry. Voltage errors are the most significant source of trajectory errors however the signal is still usable in a device with reasonably practicable random errors to electrodes, with the use of reference compounds to calibrate the mass scale.

REFERENCES

- [1] A. Makarov, "Electrostatic axially harmonic orbital trapping: A high-performance technique of mass analysis", *Analytical Chemistry*, vol. 72, pp. 1156-1162, 2000.

- [2] Q. Hu, R.J. Noll, H. Li, A. Makarov, M. Hardman, R. Graham Cooks, "The Orbitrap: a new mass spectrometer", *Journal of Mass Spectrometry*, vol. 40, pp. 430-443, 2005.
- [3] K. Richardson, J. Hoyes, "A novel multipass oa-TOF mass spectrometer", *International Journal of Mass Spectrometry*, vol. 377, pp. 309-315, 2015.
- [4] D. Manura and D. Dahl, "SIMION (R) v8.1.1", Scientific Instrument Services, Inc., <https://simion.com/>, 2013.
- [5] D. Dahl, "Simion for the personal computer in reflection", *International Journal of Mass Spectrometry*, vol. 200, pp. 3-25, 2000.